

NONLINEAR SMALL-SCALE DYNAMOS AT LOW MAGNETIC PRANDTL NUMBERS

AXEL BRANDENBURG

NORDITA, AlbaNova University Center, Roslagstullsbacken 23, SE-10691 Stockholm, Sweden; brandenb@nordita.org

AND

Department of Astronomy, Stockholm University, SE-10691 Stockholm, Sweden

Received 2011 June 28; accepted 2011 September 27; published 2011 October 21

ABSTRACT

Saturated small-scale dynamo solutions driven by isotropic non-helical turbulence are presented at low magnetic Prandtl numbers Pr_M down to 0.01. For $Pr_M < 0.1$, most of the energy is dissipated via Joule heat and, in agreement with earlier results for helical large-scale dynamos, kinetic energy dissipation is shown to diminish proportional to $Pr_M^{1/2}$ down to values of 0.1. In agreement with earlier work, there is, in addition to a short Golitsyn $k^{-11/3}$ spectrum near the resistive scale, also some evidence for a short k^{-1} spectrum on larger scales. The rms magnetic field strength of the small-scale dynamo is found to depend only weakly on the value of Pr_M and decreases by about a factor of two as Pr_M is decreased from 1 to 0.01. The possibility of dynamo action at $Pr_M = 0.1$ in the nonlinear regime is argued to be a consequence of a suppression of the bottleneck seen in the kinetic energy spectrum in the absence of a dynamo and, more generally, a suppression of kinetic energy near the dissipation wavenumber.

Key words: magnetohydrodynamics (MHD) – turbulence

Online-only material: color figure

1. INTRODUCTION

In astrophysical turbulence, dissipation of kinetic and magnetic energies tends to occur on length scales much shorter than the scale of the energy-carrying eddies. Even though both kinetic and magnetic dissipation scales are comparatively short, the current indications are that it does matter which of the two is the shorter one and by how much. Their ratio is the magnetic Prandtl number, Pr_M . For stars and liquid metals we have $Pr_M \ll 1$, while for galaxies $Pr_M \gg 1$. An important example where the value of Pr_M is believed to matter is the small-scale dynamo that converts kinetic turbulent energy into magnetic energy under isotropic conditions.

A dynamo is only possible when the energy conversion is efficient and larger than the magnetic energy dissipation. This is quantified by the magnetic Reynolds number, Re_M , which is a nondimensional measure of the inverse magnetic dissipation rate. The critical value of Re_M , above which dynamo action occurs, is known to increase with decreasing values of Pr_M (Rogachevskii & Kleeorin 1997; Boldyrev & Cattaneo 2004; Haugen et al. 2004; Schekochihin et al. 2004, 2005, 2007; Isakov et al. 2007). In the following we define the magnetic Reynolds number as $Re_M = u_{\text{rms}}/\eta k_f$, where u_{rms} is the rms velocity fluctuation of the turbulence, η is the magnetic diffusivity, and k_f is the wavenumber of the energy-carrying eddies, i.e., the wavenumber where energy is injected into the system. The critical value of Re_M is then found to be around 35 for $Pr_M = 1$ and around 100 for $Pr_M = 0.2$, but note that for Schekochihin et al. (2004, 2005, 2007) and Isakov et al. (2007) the values of Re_M are defined such that they are about 1.5 times larger than those used here or in Haugen et al. (2004). For $Pr_M = 0.1$, however, no small-scale dynamo action has yet been found. This may easily be a limitation of not having been able to increase the fluid Reynolds number, $Re = Re_M/Pr_M$, beyond 2000, which limits Re_M to 200 for $Pr_M = 0.1$ (Isakov et al. 2007; Schekochihin et al. 2007). Larger values of Re have been possible by using hyperviscosity, giving access to larger values of Re and smaller values of Pr_M for fixed Re_M . In that case, Isakov et al. (2007) and Schekochihin et al. (2007) found

small-scale dynamo action for $Pr_M = 0.05$ and $Re_M = 150$, i.e., the dynamo is now easier to excite than for $Pr_M = 0.1$. The reason for this is believed to be connected with the fact that the properties of small-scale dynamos depend on the kinetic energy spectrum at the resistive scale. For $Pr_M = 1$, this scale is the viscous scale where the velocity field is smooth in the sense that the velocity difference δu over a separation $\delta \ell$ scales linearly, i.e., $\delta u \sim \delta \ell$. For $Pr_M \ll 1$, following the argument of Boldyrev & Cattaneo (2004), the resistive scale falls in the inertial range where the velocity field is rough and $\delta u \sim \delta \ell^\zeta$ with $\zeta \approx 0.4$, so the velocity field would not be differentiable, making dynamo action inefficient. However, for $Pr_M = 0.1$, the kinetic energy spectrum is even shallower than in the inertial range, so the local value of ζ is even smaller and the velocity field rougher than in the inertial range. This phenomenon is known as the bottleneck effect (Falkovich 1994; Kaneda et al. 2003; Dobler et al. 2003). This bottleneck effect is believed to be the reason why $R_{\text{m,crit}}$ reaches a maximum at $Pr_M \approx 0.1$.

The usage of hyperviscosity does exaggerate the bottleneck, which still exists even for the regular viscosity operator. It would therefore be useful to verify small-scale dynamo action for small values of Pr_M using the regular viscosity operator. This will be done in the present paper. In addition, we shall consider here the nonlinear regime, which has the advantage that at small values of Pr_M , much of the kinetic energy is diverted to magnetic energy before it is dissipated viscously. This allows one to increase the fluid Reynolds number beyond the maximal value that would normally be possible at a given resolution. This has been demonstrated in the context of helicity-driven large-scale dynamos (Brandenburg 2009), whose onset conditions are essentially independent of the value of Pr_M (Brandenburg 2001, 2009; Mininni 2007). This is not the case for the small-scale dynamos considered here, where the flow is statistically isotropic and non-helical.

Our strategy for reaching low values of Pr_M is the same as that of Brandenburg (2009). We start with a simulation of a saturated small-scale dynamo at $Pr_M = 1$ and then increase the value of Re while keeping the value of Re_M in the range 150–160, provided the dynamo is still excited. As in Brandenburg (2009),

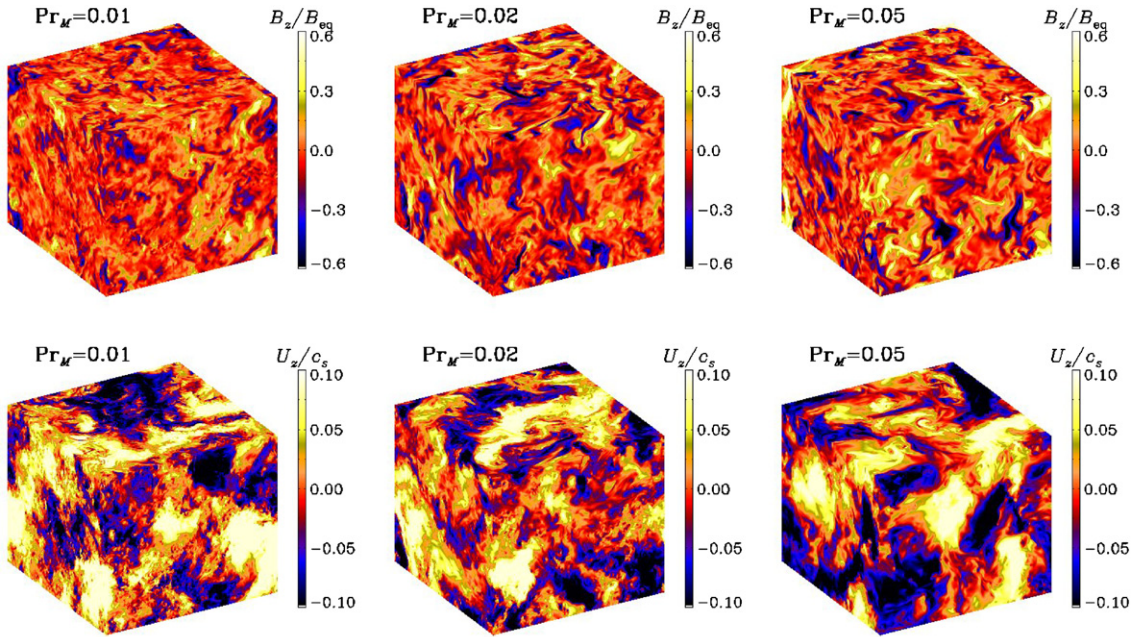


Figure 1. Visualizations of B_z and U_z for $\text{Pr}_M = 0.01$ (left), $\text{Pr}_M = 0.02$ (middle), and $\text{Pr}_M = 0.05$ (right). All runs are for $\text{Re}_M \approx 160$ using 512^3 mesh points. (A color version of this figure is available in the online journal.)

only a small fraction of the energy is dissipated viscously, which allows us then to increase Re further. We are here particularly interested in the dependence of the saturation field strength on Pr_M and the dissipation rate.

2. THE MODEL

Our model is similar to that presented in Brandenburg (2001, 2009) and Haugen et al. (2003, 2004), where we solve the hydromagnetic equations for velocity \mathbf{U} , density ρ , and magnetic vector potential \mathbf{A} , in the presence of an externally imposed non-helical forcing function \mathbf{f} , for an isothermal gas with constant sound speed c_s , i.e.,

$$\frac{\partial \mathbf{U}}{\partial t} = -\mathbf{U} \cdot \nabla \mathbf{U} - c_s^2 \nabla \ln \rho + \mathbf{f} + (\mathbf{J} \times \mathbf{B} + \nabla \cdot 2\rho \nu \mathbf{S})/\rho, \quad (1)$$

$$\frac{\partial \ln \rho}{\partial t} = -\mathbf{U} \cdot \nabla \ln \rho - \nabla \cdot \mathbf{U}, \quad (2)$$

$$\frac{\partial \mathbf{A}}{\partial t} = \mathbf{U} \times \mathbf{B} - \eta \mu_0 \mathbf{J}. \quad (3)$$

Here, $\mathbf{S}_{ij} = \frac{1}{2}(U_{i,j} + U_{j,i}) - \frac{1}{3}\delta_{ij}\nabla \cdot \mathbf{U}$ is the traceless rate of strain tensor, ν is the kinematic viscosity, $\mathbf{B} = \nabla \times \mathbf{A}$ is the magnetic field, $\mathbf{J} = \nabla \times \mathbf{B}/\mu_0$ is the current density, and μ_0 is the vacuum permeability. We consider a triply periodic domain of size L^3 , so the smallest wavenumber in the domain is $k_1 = 2\pi/L$. The forcing function consists of plane waves with wavevectors \mathbf{k} whose lengths lie in the range $1 \leq |\mathbf{k}|/k_1 \leq 2$ with an average of $k_f \approx 1.5 k_1$. The amplitude of \mathbf{f} is such that the Mach number is $u_{\text{rms}}/c_s \approx 0.1$, so compressive effects are negligible (Dobler et al. 2003).

Unless a simulation has been restarted from a previous one at another value of Pr_M , we start with a weak Gaussian distributed field in all three components of \mathbf{A} , zero initial velocity, and uniform initial density, $\rho = \rho_0 = \text{constant}$, so the volume-averaged density remains constant, i.e., $\langle \rho \rangle = \rho_0$.

In our simulations we vary the fluid Reynolds number and the magnetic Prandtl number,

$$\text{Re} = u_{\text{rms}}/\nu k_f, \quad \text{Pr}_M = \nu/\eta, \quad (4)$$

such that $\text{Re}_M = u_{\text{rms}}/\eta k_f$ is in the range 150–160. We also present a few results for Re_M around 220. We monitor the resulting kinetic and magnetic energy dissipation rates per unit volume,

$$\epsilon_K = \langle 2\nu\rho\mathbf{S}^2 \rangle, \quad \epsilon_M = \langle \eta\mu_0\mathbf{J}^2 \rangle, \quad (5)$$

whose sum, $\epsilon_T = \epsilon_K + \epsilon_M$, is the total dissipation rate. We use the fully compressible PENCIL CODE¹ for all our calculations. We recall that, for the periodic boundary conditions under consideration, $\langle 2\mathbf{S}^2 \rangle = \langle \mathbf{W}^2 \rangle + \frac{4}{3}\langle (\nabla \cdot \mathbf{U})^2 \rangle$, highlighting thus the analogy between vorticity $\mathbf{W} = \nabla \times \mathbf{U}$ and \mathbf{J} in the incompressible and weakly compressible cases.

3. RESULTS

3.1. Small-scale Magnetic and Velocity Features at Low Pr_M

In Figure 1 we present visualizations of B_z and U_z on the periphery of the domain for three runs with Pr_M ranging from 0.01 to 0.05. Even though the value of Re_M is the same in all three runs, the magnetic field seems to have smaller scale structures in the low- Pr_M case. The appearance of smaller scale structures is particularly clear in the visualization of the velocity field for $\text{Pr}_M = 0.01$.

In Table 1 we summarize some essential properties of the simulations for a sequence of simulations with different values of Pr_M between 0.01 and 1, but similar values of Re_M of around 150–160. The rms field strength relative to the equipartition value, $B_{\text{eq}} = u_{\text{rms}}\sqrt{\rho_0\mu_0}$, is about 0.3 for $0.05 \leq \text{Pr}_M \leq 0.2$, while for the runs with $\text{Pr}_M = 0.02$ and 0.01 it is about 0.15 and 0.12, respectively. This is still a remarkably weak dependence that was not expected based on the earlier results of Isakov et al. (2007) and Schekochihin et al. (2007) for the onset conditions of the small-scale dynamo. As Pr_M is decreased from 1 to 0.01, ϵ_K decreases and ϵ_M increases. However, the runs for $\text{Re}_M = 160$ are rather close to the onset of dynamo action. This becomes clear when comparing with two other runs for $\text{Re}_M = 220$, using $\text{Pr}_M = 0.1$ and 0.02; see Table 2. For $\text{Pr}_M = 0.1$,

¹ <http://www.pencil-code.googlecode.com>

Table 1
Summary of Runs for Different Values of Pr_M and $\text{Re}_M \approx 150\text{--}160$

Pr_M	Re_M	$B_{\text{rms}}/B_{\text{eq}}$	C_ϵ	ϵ_K/ϵ_T	ϵ_M/ϵ_T	k_K	k_M	$\Delta t/\tau$	Res.
0.01	163	0.12 ± 0.02	0.34 ± 0.03	0.49 ± 0.13	0.68 ± 0.06	656	28	397	512^3
0.02	163	0.15 ± 0.04	0.44 ± 0.03	0.60 ± 0.24	0.64 ± 0.10	425	29	394	512^3
0.05	157	0.28 ± 0.03	0.65 ± 0.04	0.31 ± 0.08	0.77 ± 0.05	217	31	201	512^3
0.10	158	0.28 ± 0.04	0.65 ± 0.01	0.39 ± 0.07	0.72 ± 0.04	132	31	261	256^3
0.20	152	0.32 ± 0.04	0.73 ± 0.10	0.50 ± 0.13	0.67 ± 0.05	85	30	147	256^3
0.50	150	0.39 ± 0.05	0.88 ± 0.03	0.59 ± 0.09	0.63 ± 0.04	45	30	98	256^3
1.00	146	0.39 ± 0.03	0.92 ± 0.03	0.85 ± 0.11	0.54 ± 0.03	28	29	228	256^3

Table 2
Comparison of Runs for $\text{Re}_M \approx 220$ and Two Values of Pr_M

Pr_M	$B_{\text{rms}}/B_{\text{eq}}$	C_ϵ	ϵ_K/ϵ_T	ϵ_M/ϵ_T
0.02	0.34 ± 0.02	0.70 ± 0.04	0.08 ± 0.01	0.92 ± 0.01
0.10	0.32 ± 0.03	0.66 ± 0.08	0.24 ± 0.03	0.81 ± 0.02

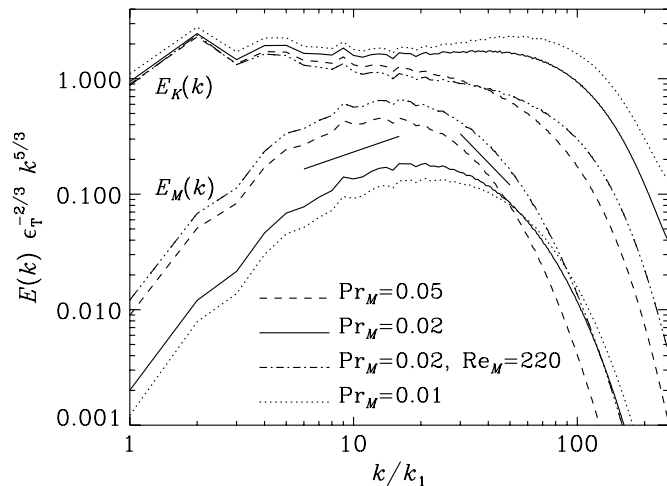


Figure 2. Compensated kinetic and magnetic energy spectra for runs with $\text{Pr}_M = 0.05$, $\text{Pr}_M = 0.02$, and $\text{Pr}_M = 0.01$ for $\text{Re}_M \approx 150$ as well as one run with $\text{Pr}_M = 0.02$ and $\text{Re}_M \approx 220$. The resolution is in all cases 512^3 mesh points. The two short straight lines give, for comparison, the slopes $2/3$ (corresponding to a k^{-1} spectrum for $k < 20k_1$) and -2 (corresponding to a $k^{-11/3}$ spectrum for $k > 20k_1$).

$B_{\text{rms}}/B_{\text{eq}} \approx 0.32$ and the ratio ϵ_K/ϵ_T has dropped from 0.39 to 0.24, while for $\text{Pr}_M = 0.02$, $B_{\text{rms}}/B_{\text{eq}} \approx 0.34$ and the ratio ϵ_K/ϵ_T has dropped from 0.6 to 0.08. Thus, we see that for values of Re_M that are not too close to the onset of dynamo action, the Pr_M dependence of $B_{\text{rms}}/B_{\text{eq}}$ is negligible and ϵ_K continues to drop.

The magnetic dissipation wavenumber, $k_M = (\epsilon_M/\eta^3)^{1/4}$, is about 30 for all runs with $\text{Re}_M \approx 150\text{--}160$, while the kinetic dissipation wavenumber, $k_K = (\epsilon_K/\nu^3)^{1/4}$, increases gradually with decreasing values of Pr_M (or increasing values of Re).

3.2. Spectral Properties and Energy Dissipation

We consider here kinetic and magnetic energy spectra, $E_K(k)$ and $E_M(k)$, respectively. They are normalized in the usual way such that $\int E_K dk = \frac{1}{2}\rho_0\langle \mathbf{U}^2 \rangle$ and $\int E_M dk = \frac{1}{2}\mu_0^{-1}\langle \mathbf{B}^2 \rangle$. In Figure 2, these spectra are compensated with $\epsilon_T^{-2/3}k^{5/3}$. For $\text{Pr}_M = 0.02$ and 0.01, the kinetic energy spectra show a clear bottleneck effect, i.e., there is a weak uprise of the compensated spectra toward the dissipative subrange (Falkovich 1994; Kaneda et al. 2003; Dobler et al. 2003). The compensated

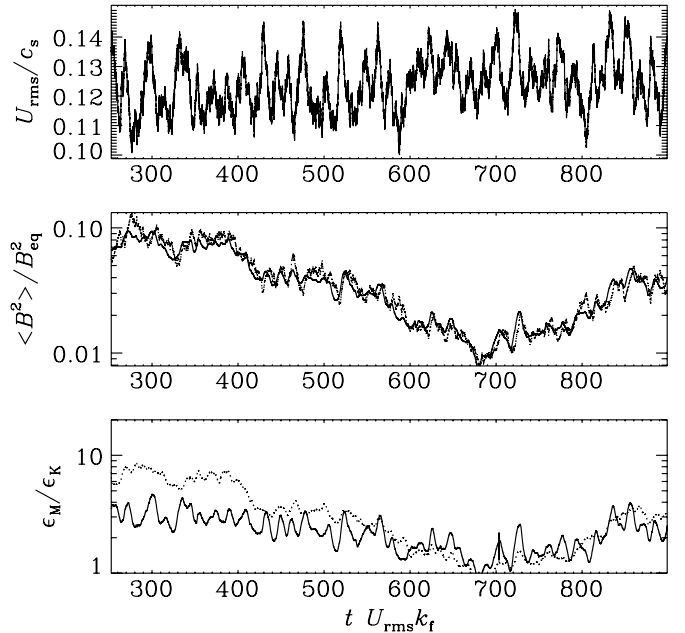


Figure 3. Root-mean-square velocity, ratio of magnetic to kinetic energy, as well as the ratio of magnetic to kinetic energy dissipation for the run with $\text{Pr}_M = 0.02$ using 512^3 mesh points. In the last two panels the dashed lines denote normalization with respect to the instantaneous values of B_{eq} and ϵ_K , respectively, while the solid lines refer to normalizations based on the time-averaged values of B_{eq} and ϵ_K .

magnetic energy spectra peak around $k = 20k_1$. Toward both larger and smaller values of k there is no clear power-law behavior. The slopes of the $k^{-11/3}$ spectrum of Golitsyn (1960) and Moffatt (1961) and the scale-invariant k^{-1} spectrum (Ruzmaikin & Shukurov 1982; Kleorin & Rogachevskii 1994; Kleorin et al. 1996) are shown for comparison.

It turns out that for small values of Pr_M , dynamo action is maintained for $\text{Re}_M \approx 160$, corresponding to $\text{Re} \approx 7800$. This value of Re is rather large for a resolution of 512^3 mesh points and one must be concerned about insufficient resolution. Similar circumstances were encountered previously in connection with simulations of large-scale dynamos at low values of Pr_M (Brandenburg 2009), and even at large values of Pr_M (Brandenburg 2011). In the former case, much of the energy dissipation occurs magnetically via Joule dissipation, thus leaving very little energy in the rest of the kinetic energy cascade. This allows us then to decrease ν further, while still allowing the remaining kinetic energy to get dissipated. However, kinetic and magnetic energies are quite intermittent (uppermost panel of Figure 3) and there can be extended periods over which the magnetic energy drops well below the kinetic

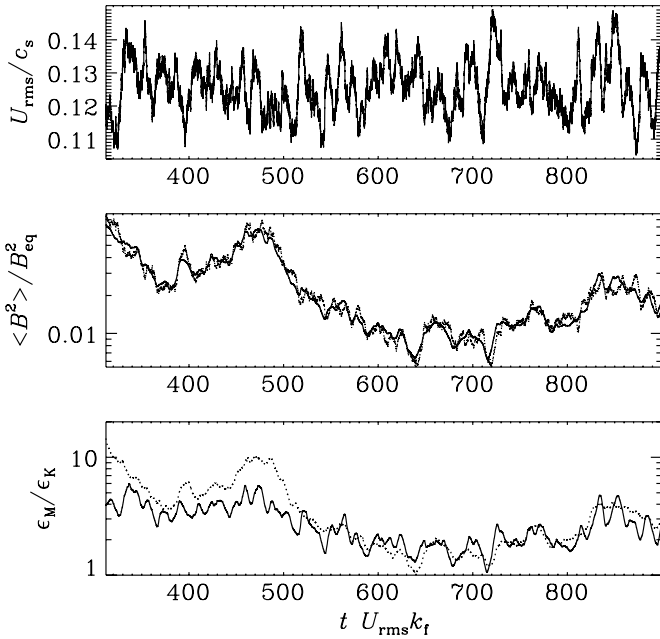


Figure 4. Same as Figure 3, but for the run with $\text{Pr}_M = 0.01$.

energy. Nevertheless, the magnetic energy dissipation is still in excess of the kinetic energy dissipation; see Figure 3.

For $\text{Pr}_M = 0.01$, the nominal value of Re is 16,000. The kinetic energy spectrum now extends further to higher wavenumbers, but it shows still a monotonic decrease down to the Nyquist wavenumber at $k = 256k_1$. As can be seen from Table 1, the nominal dissipation wavenumber, k_K , is now well outside the range of resolved wavenumbers, so it is clear that higher resolution would be needed to resolve the smallest scales properly. However, as far as the dynamo is concerned, most of the magnetic field generation occurs at wavenumbers below $30k_1$, which is where the compensated magnetic energy spectrum begins to show a clear decline into the dissipation subrange. Until that wavenumber, significant amounts of kinetic energy are being channeled into magnetic energy via the dynamo, which lowers the kinetic energy dissipation and is the main reason for being able to run such low- Pr_M cases.

The velocity field is relatively steady over the course of the simulation, but the magnetic field and also the magnetic energy dissipation vary significantly; see Figure 4. However, although there can occasionally be a dramatic decline in the magnetic field, it tends to recover subsequently, suggesting that dynamo action is still possible at small values of Pr_M . Obviously, in addition to longer run times, it is necessary to perform simulations at higher resolution, which is not currently feasible if one wants to cover sufficiently many turnover times.

We have already argued that the somewhat erratic behavior of the dynamo at $\text{Re}_M = 160$ is a consequence of being close to the marginal value. The time evolution for the case with $\text{Re}_M = 220$ and $\text{Pr}_M = 0.02$ is shown in Figure 5. Both B_{rms} and ϵ_K are now much closer to being statistically steady. Furthermore, the value of $B_{\text{rms}}/B_{\text{eq}}$ is now ≈ 0.3 both for $\text{Pr}_M = 0.1$ and for $\text{Pr}_M = 0.02$. This suggests that the saturation level of the dynamo is now beginning to be independent of the value of Pr_M .

Earlier work on large-scale dynamos from helical isotropic turbulence showed that the total magnetic energy dissipation is larger than in hydrodynamic turbulence. This is best

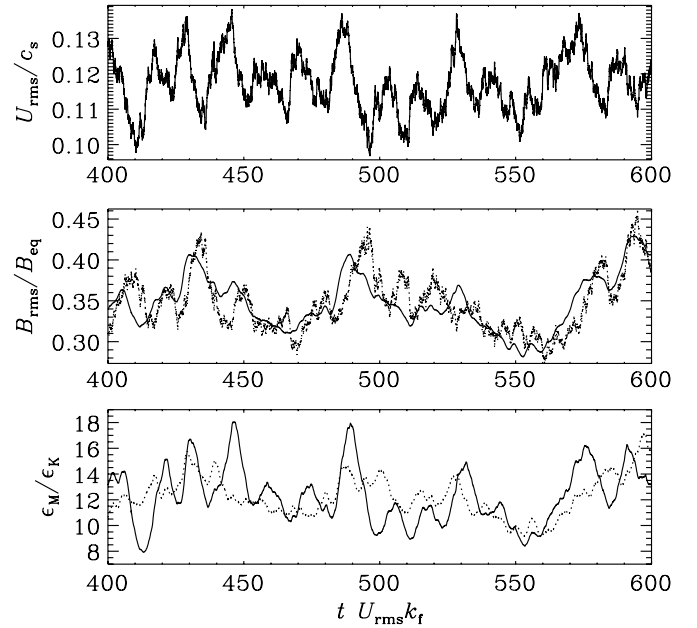


Figure 5. Similar to Figure 3, but for the run with $\text{Re}_M = 220$, still using $\text{Pr}_M = 0.02$.

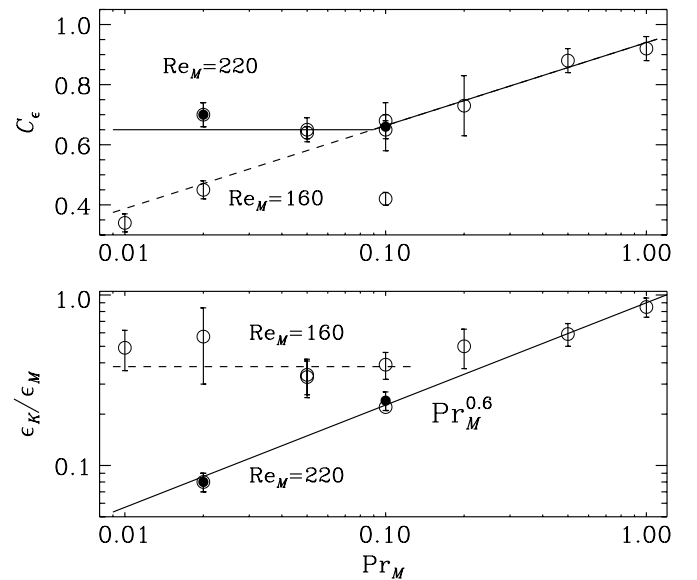


Figure 6. Pr_M dependence of the dimensionless dissipation rate, C_ϵ , and the kinetic to magnetic energy dissipation ratio, ϵ_K/ϵ_M .

demonstrated by considering the conventionally defined dimensionless dissipation parameter

$$C_\epsilon = \frac{\epsilon_T}{U^3/L}, \quad (6)$$

where U is the one-dimensional rms velocity, which is related to u_{rms} via $U^2 = u_{\text{rms}}^2/3$, and L is the integral scale which is related to k_f via $\frac{3}{4}\pi/k_f$. In non-helical turbulence this value is typically around 0.5 (see, e.g., Pearson et al. 2004), but in helical turbulence with large-scale dynamo action this value is around 1.4; see also Brandenburg (2011). In Figure 6 we use time-averaged dissipation rates, which, for simplicity, are also denoted by ϵ_K , ϵ_M , and ϵ_T . In the upper panel of Figure 6 we show that, in the present case of small-scale dynamo action from non-helical isotropic turbulence, this value is now

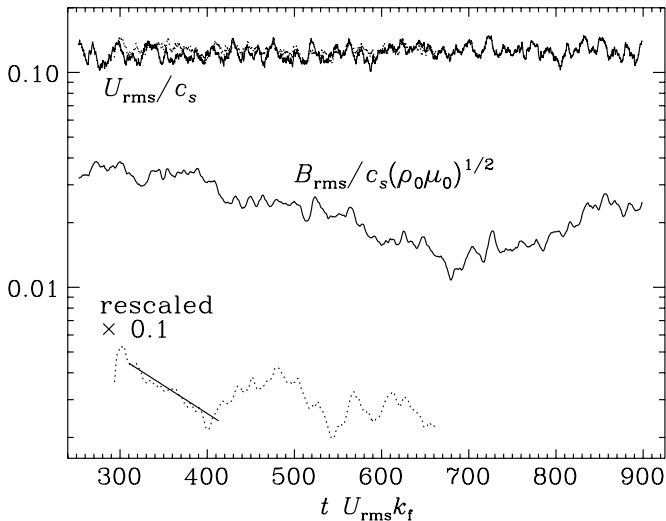


Figure 7. Evolution of magnetic and kinetic energies in the main run (solid lines) and after rescaling the magnetic field by a factor of one-tenth (dotted lines). During the first 100 turnover times, the resulting decay rate is $0.006u_{\text{rms}}k_f$.

closer to the hydrodynamic value and is slightly above 0.6 for $\text{Pr}_M = 0.02$ and $\text{Re}_M = 220$; see the upper panel of Figure 6. In the lower panel of Figure 6 we see that the ratio ϵ_K/ϵ_M is compatible with a $\text{Pr}_M^{0.6}$ dependence, as was found earlier for helical hydromagnetic turbulence (Brandenburg 2009, 2011). However, for $\text{Re}_M = 160$, ϵ_K/ϵ_M levels off at a constant value of ≈ 0.4 , which is probably an artifact of Re_M being too close to the onset of dynamo action.

3.3. Possibility of Subcritical Dynamo Action

We recall that we have used here the strategy of generating low- Pr_M solutions by gradually decreasing ν , and hence increasing the value of Re . As in the case of helical dynamos (Brandenburg 2009), the fact that a turbulent self-consistently generated magnetic field is present helps in reaching these low- Pr_M solutions. However, the presence of the magnetic field also modifies the kinetic energy spectrum and makes it decline slightly more steeply than in the absence of a magnetic field; see Figure 2. This suggests that the velocity field would be less rough than in the corresponding case without magnetic fields. Following the reasoning of Boldyrev & Cattaneo (2004), this should make the dynamo more easily excited than in the kinematic case with an infinitesimally weak magnetic field. In other words, there is the possibility of a subcritical bifurcation where the dynamo requires a significantly larger value of Pr_M to bifurcate from the trivial $\mathbf{B} = \mathbf{0}$ solution than the value needed to sustain a saturated dynamo.

In order to check this hypothesis, we perform an experiment where the simulation is continued after having downscaled the magnetic field by a factor of 10. The result is shown in Figure 7, where we compare the original simulation with the one restarted with a 10 times lower field. One sees a gradual decline of the magnetic field after a brief initial increase of the magnetic field. This initial increase is a consequence of the reduced feedback from the Lorentz force, allowing the velocity to increase slightly above the previous value (see the upper dotted line in Figure 7). During the next 100 turnover times, the decay rate is about $0.006u_{\text{rms}}k_f$, which is about four times smaller than the growth rate of $0.025u_{\text{rms}}k_f$ for a non-helical dynamo at $\text{Pr}_M = 1$ and $\text{Re} \approx 150$ (Haugen et al. 2004). However, the field still seems to recover and shows in the end a behavior comparable to that

without rescaling. This may suggest that at this value of Pr_M the dynamo may not be subcritical after all.

The possibility of subcritical dynamo action is well known in the geodynamo context, where the flow is driven by thermal or compositional convection (Roberts 1988), and for Keplerian shear flows (Rincon et al. 2008). Also in the context of dynamos from forced Taylor–Green flows the possibility of subcritical dynamos is well known (Ponty et al. 2007). In the present context, subcriticality is likely to be linked to the steeper kinetic energy spectrum in the low- Pr_M regime. However, because of extended transients, the results for $\text{Pr}_M = 0.02$ shown in Figure 7 remain inconclusive. For $\text{Pr}_M = 0.1$, on the other hand, Schekochihin et al. (2007) have not seen dynamo action in the linear regime when $\text{Re}_M = 160$.

4. CONCLUSIONS

In the present paper we have extended the work of Isakov et al. (2007) and Schekochihin et al. (2007) to the nonlinear regime of a saturated dynamo. However, while in the former (linear) case the dynamo shows signs of a depression in the range $0.1 \leq \text{Pr}_M \leq 0.2$, the nonlinear saturated dynamo is found to operate almost unimpeded in the range $0.02 \leq \text{Pr}_M \leq 1$. Furthermore, unlike the work of Isakov et al. (2007) and Schekochihin et al. (2007), who used hyperviscosity, we have here used regular viscosity with the usual Laplacian diffusion operator. As in earlier work on helical large-scale dynamos (Brandenburg 2009), it is possible to reach the regime of low Pr_M by restarting the simulations from another one at a larger value of Pr_M , which reduces the kinetic dissipation rate proportional to the square root of Pr_M . Furthermore, in contrast to helical large-scale dynamos, where dynamo onset is possible for values of Re_M of the order of unity and independently of the value of Pr_M , we have here the situation where the critical value of Re_M may be larger than the value required to sustain the dynamo once it has saturated. This means that the dynamo could be subcritical and might possess a finite amplitude instability at Re_M below and around 160.

We note that the approximate $\text{Pr}_M^{1/2}$ scaling of the kinetic to magnetic energy dissipation ratio, ϵ_K/ϵ_M , is still not well understood. In view of the definitions of ϵ_K and ϵ_M in Equation (5), it is clear that this implies that

$$\frac{\nu^{1/2} \langle \rho \mathbf{W}^2 \rangle}{\eta^{1/2} \langle \mu_0 \mathbf{J}^2 \rangle} = \text{constant} \quad (7)$$

This means that the usually expected scaling for hydrodynamic turbulence, $\nu \langle \rho \mathbf{W}^2 \rangle = \text{constant}$, or the hydromagnetic scaling $\eta \langle \mu_0 \mathbf{J}^2 \rangle = \text{constant}$, which has been confirmed for $\text{Pr}_M = 1$ (see Figure 8 of Candelaresi et al. 2011), is clearly not generally valid and needs to be reconsidered.

Our results for the magnetic energy spectra are consistent with those of earlier direct numerical simulations by Schekochihin et al. (2007) in that there is a short Golitsyn $k^{-11/3}$ spectrum near the resistive scale, as well as a short k^{-1} spectrum on larger scales. Both properties have also been seen in liquid sodium experiments (Odier et al. 1998; Bourgoin et al. 2002) as well as in large eddy simulations (Ponty et al. 2004).

The astrophysical relevance of small-scale dynamo action is hardly disputed. Even in situations where large-scale dynamo action is possible, like in the Sun, small-scale magnetic fields are seen ubiquitously even in the quiet photosphere where there is no evidence of any effects from the large-scale field (Cattaneo 1999; Vögler & Schüssler 2007; Pietarila Graham et al. 2010; Jin

et al. 2011). The present work now confirms that the small value of the Sun's magnetic Prandtl number may not be a problem with this proposal. Although one may worry that most of the simulations presented so far have overestimated the effects of small-scale dynamo action by having chosen values of Pr_M of the order of unity (Brandenburg 2005), it is remarkable that the field strength decreases only slightly when we decrease Pr_M from 1 to 0.02, provided Re_M is large enough ($\text{Re}_M \gtrsim 150$). Future work will hopefully clarify further the relative importance of large-scale and small-scale dynamo action in astrophysical bodies like the Sun.

Another aspect that needs to be addressed in future simulations concerns the magnetic Prandtl number effects on the large-scale properties of the turbulence. This concerns in particular the turbulent diffusion of large-scale magnetic fields, as can be measured by the quasi-kinematic test-field method, for example (Brandenburg et al. 2008). Among other things, one would like to confirm that the turbulent magnetic diffusivity is not affected by the small-scale magnetic field, which is a standard result in mean-field theory (Gruzinov & Diamond 1994; Rädler et al. 2003; Brandenburg & Subramanian 2005). In that case, if Re_M is close to the onset of small-scale dynamo action, one would expect the turbulent diffusion to be independent of the value of Pr_M . However, for large values of Re_M , as we have now seen, the effect of Pr_M on the small-scale dynamo is less dramatic. Thus, even if the turbulent magnetic diffusivity was affected by the small-scale field, the effect could only be weak.

I thank Paul Roberts for hospitality during a visit to Malibu where this project was started. I also acknowledge the organizers of the KITP program on turbulence for providing a stimulating atmosphere. This research was supported in part by the National Science Foundation under grant PHY05-51164 and the European Research Council under the AstroDyn Research Project 227952. The computations have been carried out at the National Supercomputer Centre in Umeå and at the Center for Parallel Computers at the Royal Institute of Technology in Sweden.

REFERENCES

- Boldyrev, S., & Cattaneo, F. 2004, *Phys. Rev. Lett.*, **92**, 144501
 Bourgoin, M., Marié, L., Pétrélis, F., et al. 2002, *Phys. Fluids*, **14**, 3046

- Brandenburg, A. 2001, *ApJ*, **550**, 824
 Brandenburg, A. 2005, *ApJ*, **625**, 539
 Brandenburg, A. 2009, *ApJ*, **697**, 1206
 Brandenburg, A. 2011, *Astron. Nachr.*, **332**, 51
 Brandenburg, A., Rädler, K.-H., Rheinhardt, M., & Subramanian, K. 2008, *ApJ*, **687**, L49
 Brandenburg, A., & Subramanian, K. 2005, *Phys. Rep.*, **417**, 1
 Candelaresi, S., Hubbard, A., Brandenburg, A., & Mitra, D. 2011, *Phys. Plasmas*, **18**, 012903
 Cattaneo, F. 1999, *ApJ*, **515**, L39
 Dobler, W., Haugen, N. E. L., Yousef, T. A., & Brandenburg, A. 2003, *Phys. Rev. E*, **68**, 026304
 Falkovich, G. 1994, *Phys. Fluids*, **6**, 1411
 Golitsyn, G. S. 1960, *Sov. Phys.—Dokl.*, **5**, 536
 Gruzinov, A. V., & Diamond, P. H. 1994, *Phys. Rev. Lett.*, **72**, 1651
 Haugen, N. E. L., Brandenburg, A., & Dobler, W. 2003, *ApJ*, **597**, L141
 Haugen, N. E. L., Brandenburg, A., & Dobler, W. 2004, *Phys. Rev. E*, **70**, 016308
 Iskakov, A. B., Schekochihin, A. A., Cowley, S. C., McWilliams, J. C., & Proctor, M. R. E. 2007, *Phys. Rev. Lett.*, **98**, 208501
 Jin, C. L., Wang, J. X., Song, Q., & Zhao, H. 2011, *ApJ*, **731**, 37
 Kaneda, Y., Ishihara, T., Yokokawa, M., Itakura, K., & Uno, A. 2003, *Phys. Fluids*, **15**, L21
 Kleorin, N., Mond, M., & Rogachevskii, I. 1996, *A&A*, **307**, 293
 Kleorin, N., & Rogachevskii, I. 1994, *Phys. Rev. E*, **50**, 2716
 Mininni, P. D. 2007, *Phys. Rev. E*, **76**, 026316
 Moffatt, H. K. 1961, *J. Fluid Mech.*, **11**, 625
 Odier, P., Pinton, J.-F., & Fauve, S. 1998, *Phys. Rev. E*, **58**, 7397
 Pearson, B. R., Yousef, T. A., Haugen, N. E. L., Brandenburg, A., & Krogstad, P. Å. 2004, *Phys. Rev. E*, **70**, 056301
 Pietarila Graham, J., Cameron, R., & Schüssler, M. 2010, *ApJ*, **714**, 1606
 Ponty, Y., Laval, J.-P., Dubrulle, B., Daviaud, F., & Pinton, J.-F. 2007, *Phys. Rev. Lett.*, **99**, 224501
 Ponty, Y., Politano, H., & Pinton, J.-F. 2004, *Phys. Rev. Lett.*, **92**, 144503
 Rädler, K.-H., Kleorin, N., & Rogachevskii, I. 2003, *Geophys. Astrophys. Fluid Dyn.*, **97**, 249
 Rincon, F., Ogilvie, G. I., Proctor, M. R. E., & Cossu, C. 2008, *Astron. Nachr.*, **329**, 750
 Roberts, P. H. 1988, *Geophys. Astrophys. Fluid Dyn.*, **44**, 3
 Rogachevskii, I., & Kleorin, N. 1997, *Phys. Rev. E*, **56**, 417
 Ruzmaikin, A. A., & Shukurov, A. M. 1982, *Ap&SS*, **82**, 397
 Schekochihin, A. A., Cowley, S. C., Taylor, S. F., Maron, J. L., & McWilliams, J. C. 2004, *ApJ*, **612**, 276
 Schekochihin, A. A., Haugen, N. E. L., Brandenburg, A., et al. 2005, *ApJ*, **625**, L115
 Schekochihin, A. A., Iskakov, A. B., Cowley, S. C., et al. 2007, *New J. Phys.*, **9**, 300
 Vögler, A., & Schüssler, M. 2007, *A&A*, **465**, L43